Dimerization of Human XPA and Formation of XPA_2−RPA Protein Complex†

Zheng-guan Yang,‡ Yang Liu,§ Leslie Y. Mao,‡ Jian-Ting Zhang,§ and Yue Zou*,‡

Department of Biochemistry and Molecular Biology, James H. Quillen College of Medicine, East Tennessee State University, Johnson City, Tennessee 37614, and Department of Pharmacology/Toxicology, Walther Cancer Institute/Walther Oncology Center, and IU Cancer Center, Indiana University School of Medicine, Indianapolis, Indiana 46202

Received May 2, 2002; Revised Manuscript Received August 3, 2002

ABSTRACT: XPA plays an important role in the DNA damage recognition during human nucleotide excision repair. Here we report that the XPA is a homodimer either in the free state or as a complex with human RPA in solution under normal conditions. The human XPA protein purified from baculovirus-infected sf21 insect cells has a molecular mass of 36 317 Da, as determined by mass spectroscopy. However, the apparent molecular mass of XPA determined by the native gel filtration chromatography was about 71 kDa, suggesting that XPA is a dimer. This observation was supported by a native PFO−PAGE and fluorescence spectroscopy analysis. XPA formed a dimer (XPA_2) in a broad range of XPA and NaCl concentrations, and the dimerization was not due to the disulfide bond formation. Furthermore, a titration analysis of the binding of XPA to the human RPA indicated that it was the XPA_2 that formed the complex with RPA. Finally, the difference between the mass spectrometric and the calculated masses of XPA implies that the protein contains posttranslational modifications. Taken together, our data suggest that the dimerization of XPA may play an important role in the DNA damage recognition of nucleotide excision repair.

The human XPA (xeroderma pigmentosum group A) protein is an indispensable participant of human nucleotide excision repair (NER)[1] that recognizes and removes a large variety of bulky DNA lesions, which are structurally and chemically distinct (*1*, *2*). The XPA gene is required for both global genome repair (GGR) and transcription-coupled repair (TCR) (*3*, *4*). The protein with a zinc finger motif is capable of binding specifically to damaged DNA in vitro. In the mechanism of human NER, XPA interacts with the replication protein A (RPA) which also recognizes bulky DNA damage, to form a tight protein−protein complex. It is believed that this complex is involved in the DNA damage recognition process at the early steps of NER, and it also plays a role in the NER complex and nuclease assembly (*5*−*7*).

Because of the importance of XPA in both the damage recognition and assembly of NER, the interactions of XPA with DNA and other NER proteins have been widely studied. It has been suggested that the involvement of XPA in the DNA damage recognition is primarily determined by its efficient binding to rigidly bent DNA duplexes (*8*). This binding potential integrated with the damage recognition power of RPA through the formation of XPA−RPA complex delivers enhanced affinity for DNA lesions (*9*, *10*). The XPC−HR23B is the other important protein complex involved in the DNA damage recognition. The XPC−HR23B is generally believed to be involved in the initial DNA damage recognition in GGR, which is probably followed by the further recognition of the damage by XPA−RPA (*11*, *36*). In TCR where the XPC−HR23B may not be required, the RNA polymerase complex may play a substituting role for initial damage finding. Compared to the XPC−HR23B, the exclusive roles of XPA in NER are demonstrated by its indispensable involvement in both the GGR and the TCR for DNA damage recognition and its presence in the final excision complex.

The XPA has been generally considered to be a monomer under physiological conditions, either in its free state or as complex with DNA, RPA, or other proteins in NER. No solid evidence has been presented to show the actual form of XPA. It is clear that knowledge of the aqueous form of XPA protein is important for determination of the protein's structure, biochemical characteristics, and interactions with DNA and other proteins, and therefore, the mechanism of nucleotide excision repair including the damage recognition.

In the present study, we examined the possibility of self-association of XPA and the interaction with its closest NER partner RPA. The human XPA proteins were overproduced and purified from eukaryotic cells. Using a combination of gel filtration, perfluoro-octanoic acid (PFO) native PAGE methods, and a protein−protein binding assay, we demonstrated that XPA forms tightly a homodimer under the normal experimental conditions, which was also supported by a study of fluorescence spectroscopy of the protein. Our further titration analysis of RPA with XPA showed that XPA

† This study was supported by National Institutes of Health NCI Grants CA86927 (to Y.Z.) and CA64539 (to J.T.Z.).

* To whom correspondence should be addressed. Phone: (423) 439-7179. Fax: (423) 439-8235. E-mail: zouy@etsu.edu.

‡ East Tennessee State University.

§ Indiana University School of Medicine.

[1] Abbreviations: AAF, *N*-acetyl-2-aminofluorene; BPDE, benzo[*a*]-pyrene diol epoxide, (7,8-dihydroxy-9,10-epoxy-7,8,9,10-tetra-hydrobenzo-[*a*]pyrene); GGR, global genome repair; IPTG, isopropylthio-β-D-galactoside; MS, mass spectroscopy; NER, nucleotide excision repair; PAGE, polyacrylamide gel electrophoresis; PFO, perfluoro-octanoic acid; TCA, trichloroacetic acid; TCR, transcription-coupled repair.

10.1021/bi026064z CCC: $22.00
Published on Web 10/05/2002

interacts with RPA and forms the XPA_2−RPA heterotrimer protein complex. Finally, in comparison with the calculated molecular mass of XPA, the MS data implied that human XPA contains posttranslational modifications.

EXPERIMENTAL PROCEDURES

Human XPA and RPA Purifications. The $[His]_6$-XPA was purified from the sf21 cells infected with recombinant baculovirus pBac-XPA (graciously provided by J. J. Turchi, Wright State University School of Medicine), as described previously (*14*). Briefly, 2 L of sf21 cells at a density of 1×10^6 cells/mL in a spinner flask were infected with the recombinant virus at a multiplicity of infection (moi) of 10. After 48 h infection, the cells were harvested by centrifugation at 2000*g* for 10 min and washed twice with PBS. The cells resuspended in the buffer A (20 mM Tris, pH 7.4, 1 mM imidazole, and 0.5 M NaCl) were then lysed by sonication. All the buffers used in the purification were supplemented with protease inhibitors (0.5 mM PMSF, 1 μg/mL leupeptin, and 1 μg/mL pepstatin). After centrifugation at 13000*g* for 1 h at 4 °C, the supernatant was mixed with 4 mL of Ni-NTA Superflow resin equilibrated with buffer A, followed by incubation at 4 °C on a rotator overnight. After the incubation, the resin was used for making a column and washed twice with 100 mL of buffer A with 1 mM imidazole and then twice with 5 mM imidazole. Proteins were eluted in buffer A with 200 mM imidazole. Fractions containing the $[His]_6$-XPA protein were pooled and dialyzed into buffer B containing 50 mM Tris, pH 7.5, 0.1 M NaCl, 1 mM DTT, 1 mM EDTA, and 20% glycerol. In the final step, the XPA in the dialyzed fractions was separated from other contaminants on a 6 mL of Heparin-Sepharose column equilibrated with buffer B containing 0.1 M NaCl. The XPA protein was eluted using a 250 mL of NaCl gradient (0.1 to 1 M) in buffer B. Fractions containing XPA were pooled and concentrated using Amicon filter centrifuged at 2500*g* for 1 h at 4 °C, followed by dialysis against buffer B containing 0.1 M NaCl. The purified XPA in 200 μL aliquots were stored at −80 °C. The concentration of XPA protein was determined using Bio-Rad Protein Assay Kit.

RPA was purified in one step through a 14 mL chitin column from *Escherichia coli* strain BL-21(DE3)-RP (Stratagene) transformed with the overexpressing plasmid pTYB−RPA containing the RPA cDNA under the control of the IPTG-induced T7 promoter. The pTYB−RPA was constructed by subcloning the RPA cDNA from plasmid p11d-tRPA (graciously supplied by M. S. Wold, University of Iowa College of Medicine) into the pTYB2 vector (New England BioLabs). Briefly, the RPA cDNA in p11d-tRPA was amplified by PCR with *Pfu* DNA polymerase (Stratagene) and two primers containing a *Nde*I and a *Sma*I sites, respectively, which flank the gene. The PCR products were purified with a PCR purification kit (Qiagen) by following the procedures suggested by the manufacturer. Both the PCR-purified product and the vector pTYB2 were subjected to restriction with *Nde*I and *Sma*I. After purification, the restricted vector pTYB2 was dephosphorylated by alkaline phosphatase for increasing the subsequent ligation efficiency. The products were purified again for the ligation in which the dephosphorylated vector (3.5 ng) and the purified PCR-generated RPA cDNA fragment (0.4 ng) were incubated with 10 units of T4 DNA ligase (Gibco) in 60 μL of ligation buffer at 16 °C for 12 h, then at 37 °C for 1 h. One-twentieth of the ligation products were then transformed into competent *E. coli* DH5α cells (Gibco). The cells were plated and selected against 100 μg/mL ampicillin. Colonies were screened for those containing the plasmid encoding the RPA cDNA by both restriction and PCR assays. The final construct was confirmed by full-length DNA sequencing. It should be noted that the cloning into the *Sma*I site left an additional glycine residue attached to the C-terminus of the p32 subunit of RPA protein.

To purify RPA, the transformed *E. coli* BL21(DE3)-RP cells with pTYB−RPA were plated on LB-agar with 100μg/mL ampicillin. A freshly grown colony was inoculated into 4 mL of LB with 100 μg/mL ampicillin and 50 μg/mL chloramphenicol. The culture with high density was transferred into 4 L of LB supplemented with 100 μg/mL ampicillin. IPTG (isopropylthio-β-D-galactoside) was added to a final concentration of 1.0 mM for induction for 3 h at 25 °C after the OD (600 nm) of the culture reached 0.6. The cells were harvested and centrifuged at 5000*g* for 10 min at 4 °C. The pellets were re-suspended in ice cold column buffer (20 mM Tris-HCl pH 8.0, 1 M NaCl, 0.1 mM EDTA, 0.1% Triton X-100) and lysed by sonication on ice. Supernatants were obtained by centrifugation at 12000*g* for 30 min at 4 °C, and loaded on a chitin beads column (New England Biotech) that was preequilibrated with the column buffer. Column was washed with 200 mL of the buffer containing 30 mM HEPES pH 7.8, 0.25 mM EDTA, 0.01% NP-40, 1 mM DTT, 10% glycerol, and 0.8 M NaSCN. The on-column cleavage of RPA from the fused intein-chitin binding domain was induced by flushing the column quickly with three column volumes of the cleavage buffer (20 mM Tris-HCl pH 8.0, 500 mM NaCl, 0.1 mM EDTA, and 30 mM DTT). The flow was stopped immediately, and the cleavage was allowed to continue overnight at 4 °C. RPA protein was eluted and collected with the cleavage buffer without DTT, and then dialyzed in storage buffer (30 mM HEPES, pH 7.8, 0.25 mM EDTA, 0.01% NP-40, 1 mM DTT, 100 mM NaCl, 50% glycerol). The concentration of RPA protein was determined using Bio-Rad Protein Assay Kit.

Gel Mobility Shift Assays. Binding of XPA protein to the DNA substrates was determined by gel mobility-shift assays. The DNA substrates used in this assay were constructed following the procedures as described previously (*34*). Two types of substrates were used, the 50 bp DNA containing a single AAF or BPDE adduct and the 50 bp DNA containing a six-base mismatched region around the adduct (bubble substrate). Typically, the substrate (3 nM) was incubated with varying concentrations of XPA or RPA at 30 °C for 10 min in 20 μL of the binding buffer (40 mM HEPES−KOH, pH 7.9, 75 mM KCl, 8 mM $MgCl_2$, 1 mM DTT, 5% glycerol, and 100 μg/mL BSA). After incubation, 2 μL of 80% (v/v) glycerol was added, and the mixture was immediately loaded onto a 3.5% native polyacrylamide gel in TBE running buffer and electrophoresed at room temperature.

Mass Spectrometry. The molecular mass of the purified XPA was determined by mass spectroscopy. Protein sample for analysis was prepared using the $ZipTip_{C18}$ pipet tips following the procedures suggested by manufacturer. The protein was eluted directly onto MALDI target in 50% ACN/0.1% TFA/matrix/water for analysis on a Voyager-DE STR (Perseptive Biosystems) mass spectrometer.

Gel Filtration Chromatograph. All the gel filtration experiments were performed on an AKTApurifier system (Amersham Pharmacia Biotech) with the Superdex-200 HR and Superdex-75 HR columns (Amersham Pharmacia Biotech). Typically, 100−200 μL proteins (XPA, RPA, or markers) were automatically injected onto the Superdex column equilibrated with the running buffer containing 50 mM Tris-HCl, pH 7.5, 1 mM DTT, 1 mM EDTA, 0.1 M NaCl, and 10% glycerol. The markers include ribonuclease A, 13.7; chymotrysinogen A, 25; ovalbumin, 43; albumin, 67; aldolase, 158; catalase, 232; ferritin, 440; thyroglobulin, 669; and blue dextran, 2000 kDa (Amersham Pharmacia Biotech). The samples were analyzed with the running buffer under the conditions with monitored UV wavelength = 280 nm, flow rate = 0.5 mL/min, loading loop volume = 100 or 200 μL, and fraction size = 1 mL. Retention time was calculated with the software UNICORN Version 3.10 supplied with the system. After each run, the proteins in the collected fractions were precipitated with 10% TCA for subsequent SDS−PAGE analysis. For the titration experiments, XPA and RPA (0.61 μM) proteins with specific molar ratio (XPA/RPA = 0, 0.5, 1, 1.5, 2, 3, 4, or 8) were premixed in running buffer and centrifuged for 5 min at 13 000 rpm, followed by the incubation for 20 min at room temperature. The mixture was then loaded to the column for analysis. To reduce the systematic errors of measurement, concentrations of XPA and RPA were determined at the same time using the Bio-Rad protein assay. The quantification was conducted by integrating the enveloped area of peaks corresponding to the specific protein molar ratios. The free XPA concentration at each titration point was evaluated by subtracting the RPA background obtained in absence of XPA from the XPA titration data. For comparison, the same experiments were also carried out for varying concentrations of XPA but in the absence of RPA. In this case, 0.1 mg/mL of ribonuclease A protein (13 700 Da, retention time, 17.05 mL) was mixed with XPA for stabilization purpose. Under the denaturing conditions, the gel filtration experiments were performed with the running buffer containing 0.1% SDS. The protein samples were first treated with 1% SDS for 10 min at room temperature and then diluted to 0.1% SDS with the running buffer.

PFO−PAGE Analysis. The PFO (Oakwood Products, West Columbia, SC) native PAGE was performed as previously described (*12*) with some minor modifications. Briefly, 2−3 μg protein samples were mixed with the same volume of 2×PFO sample buffer [100 mM Tris base, 0.2% (w/v) NaPFO, 20% (v/v) glycerol, 0.005% bromophenol blue, 25 mM DTT, pH 8.0] and then immediately loaded onto the freshly prepared 7.5% native Tris/glycine polyacrylamide gel without SDS. The running buffer contained 25 mM Tris, 192 mM glycine and 0.1% (w/v) NaPFO, at pH 8.5. All of the preparations were made at 4 °C. Electrophoresis was preformed at 100 V at 4 °C in cold room. After the electrophoresis, the gels were stained with Coomassie Blue.

Fluorescence Measurement. The tryptophan fluorescence spectra of XPA were recorded on a SPEX Fluoromax fluorometer with the excitation wavelength = 295 nm, and the slit width was set at 5 nm for both excitation and emission beams. The XPA was measured at room temperature in the buffer of 25 mM Tris, 192 mM glycine at pH 8.5, in the presence and absence of NaPFO.

Protein−Protein Binding Assay. The cDNA of human XPA, which was amplified from the pBAc−XPA, was subcloned into the pTYB4 vector (New England Biolabs) following the similar procedures as described above for pTYB−RPA construction. The constructed pTYB−XPA was then transformed into pLysS competent cell (Novagen), and plated onto LB-agar with ampicillin and chloramphenicol. As a control, the pLysS cells without transformation were also directly plated onto LB-agar without antibiotics. Freshly grown colonies from the plates were inoculated into 4 mL of LB with 100 μg/mL ampicilline and 50 μg/mL chloramphenicol (nontransformed pLysS colony with chloramphenicol only). The cultures with high density were then transferred into 200 mL of LB. IPTG (isopropylthio-β-D-galactoside) was added to a final concentration of 1 mM for induction for 6 h at 28 °C after the OD (600 nm) of the culture reached 0.6. To obtain the supernatants, cells were then treated in the same way as described earlier for RPA purification except that proteinase inhibitors aprotinin (8 mg/mL) and PMSF (0.5 μM) (both from Sigma) were added in all buffers used.

A total of 50 μL of XPA (2.7 mg/mL) purified from the pBAc−XPA infected insect cells was mixed with 10 mL of the supernatants from the pTYB−XPA transformed and nontranformed pLysS cells, respectively, followed by incubation overnight at 4 °C and then 2 h at 25 °C. Incubated mixtures were then loaded onto two 1-mL chitin-beads columns (NEB), one for the transformed and the other for the nontransformed. Eluted fractions (1 mL each) were obtained following the same procedures as for the RPA purification above. The first three fractions from each column were then subjected to a 10% SDS−PAGE electrophoresis and the Western blotting analysis as previously described (*37*). The XPA both from the pBAc−XPA and pTYB−XPA was detected in the immunoblots using a XPA monoclonal antibody (12F5 from Kamiya Biomedical Co., Seattle, WA) with a dilution ratio of 1:200 in the blocking buffer (5% nonfat dry milk and 0.1% Tween 20 in phosphate buffered saline PBS).

RESULTS

Basic Determination of Purified Human XPA and RPA. Considering the possible posttranslational modifications of XPA in cells (*13*), the XPA used in this study was overproduced in the eukaryotic cells (sf21) and purified following the procedures as described previously (*14*). As shown in Figure 1A, the homogeneous XPA was obtained from the Heparin-Sepharose column in the last step of the purification procedures (see Experimental Procedures) which produced a yield of about 1.5 mg from 1 L of infected cells. The proteins were stained with Coomassie Blue. Consistent with the previous report (*14*), the purified XPA has an apparent molecular mass of about 43 kDa as determined by the SDS−PAGE, and functionally binds to the damaged DNA (Figure 1B). Since many DNA adducts recognized by XPA induce local DNA unwinding, it is of interest to test if strand opening is one of the components required for XPA binding. The data from the XPA binding to AAF−DNA showed that XPA has a significantly higher affinity for an adduct in the double-stranded DNA than for that in the DNA bubble, suggesting that DNA strand opening may not be the alteration of DNA conformation recognized by XPA. To

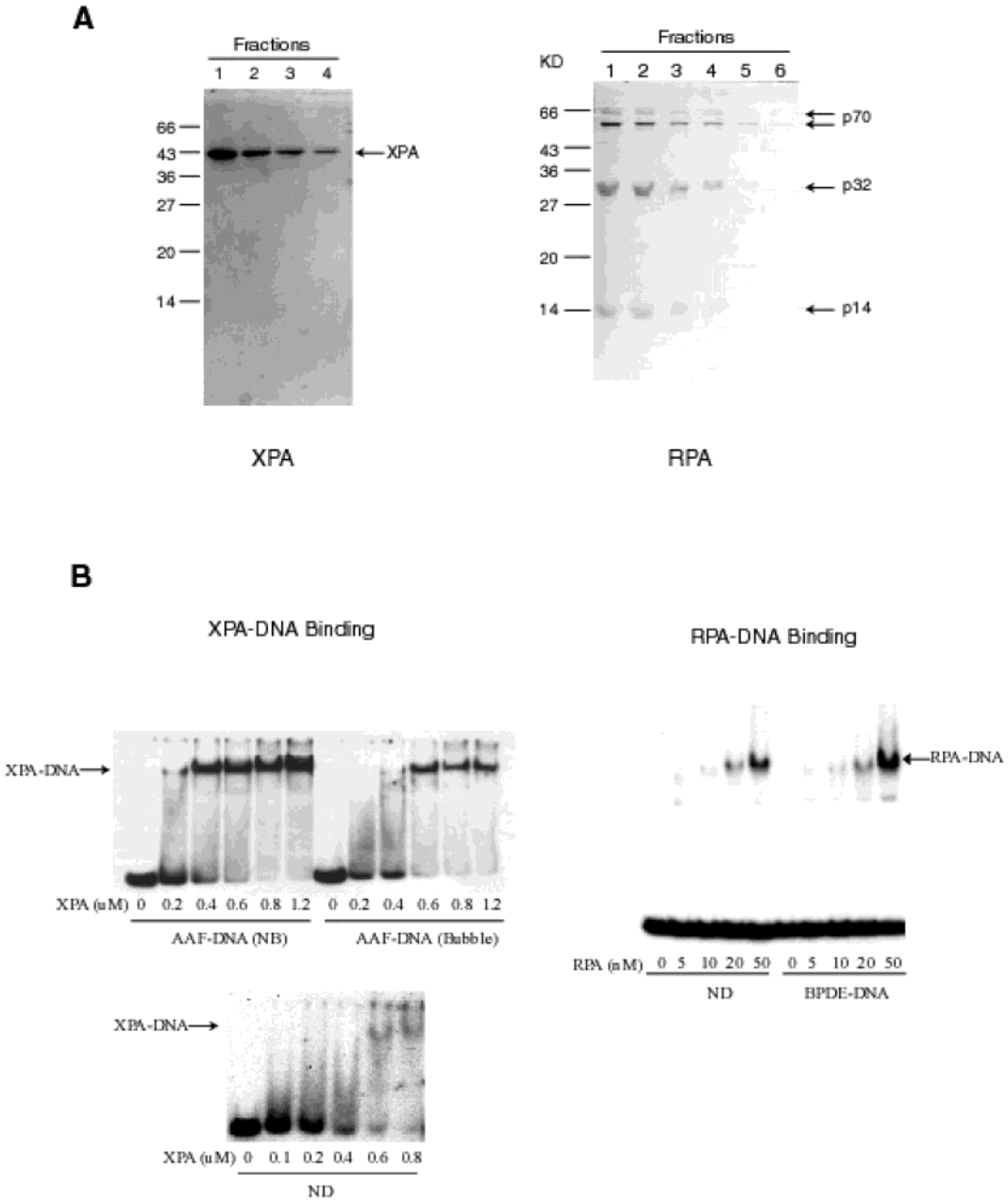

FIGURE 1: Purification of XPA and RPA proteins and their binding to DNA substrates. (A) The XPA protein was overproduced and purified from the baculovirus-infected sf21 insect cells. The RPA protein was overexpressed with the pTYB-RPA plasmid construct in *E. coli*, and purified from a chitin-binding column. Both proteins were analyzed on a 12% SDS−PAGE. The proteins were stained with Coomassie Blue. (B) The XPA or RPA at various concentrations was incubated with bubble (six-base) or nonbubble DNA substrates (50-bp) containing a single AAF or BPDE adduct in the binding buffer at 30 °C for 10 min. The ND stands for the nondamaged DNA. The samples were analyzed on a 3.5% native polyacrylamide gel.

investigate the interactions of XPA with the human RPA, the RPA was overproduced from *E. coli* transformed with the construct pTYB−RPA and purified to homogeneity using a single chitin column (Figure 1A). As shown in Figure 1B, the purified RPA was able to specifically bind to the damaged DNA. It should be noted that, although the RPA binds significantly to undamaged DNA, too (*10*, *38*), the 50 bp undamaged substrate has many more binding sites available for nonspecific binding than the damaged DNA for specific binding of a single damaged site. Therefore the affinity for the adduct was estimated to be about two orders higher than for the undamaged DNA.

To precisely determine the molecular mass of purified XPA, the mass spectroscopic analysis was conducted. The data shown in Figure 2 indicated that the insect cell-expressed XPA has a mass of 36 317 Da. This value is greater than the molecular mass of XPA calculated (36 017 Da) based on its amino acid sequence and the sequence of the tag, implying that posttranslational modifications may occur during expression of the protein in the eukaryotic cells. In comparison, the MS-determined molecular mass of XPA produced in bacteria was in a very good agreement with the calculated one (*15*). In addition to the major mass peak representing the XPA monomer, a small peak at 73 061 Da for XPA dimer was also observed. Although this dimer signal may be due to the ionization of the protein occurring during the mass measurement, it cannot be ruled out that the possible

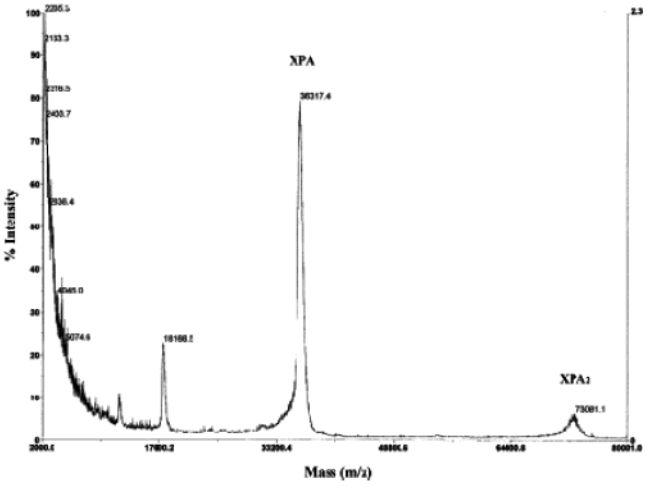

FIGURE 2: Mass spectroscopy of XPA protein. The molecular mass of XPA was measured on a Voyager-DE STR mass spectrometer (Perseptive Biosystems) using MALDI protocol. The major signal represents the XPA monomer with a molecular mass of 36 317 (*m*/*z*) where m stands for mass and *z* for the number of charges of the ionized protein. The intensity at the 73 081 (*m*/*z*) represents the XPA dimer.

original dimerization of XPA might contribute to this mass signal.

Gel Filtration Characterization. Gel filtration chromatography has been widely used for protein separation and also for determination of the size and molecular mass of proteins under native conditions. Since there is a big difference in size and molecular mass between the monomer and the oligomer of XPA (if it forms), the gel filtration technique was used for analysis of the possible self-association of XPA. As shown in Figure 3A, the gel filtration chromatography was performed for both the XPA and a wide range of molecular mass markers under the same conditions on a Superdex-200 HR column driven by the AKTApurifier system (Pharmacia Biotech). The XPA had a retention time of 13.2 mL, which was well shorter than the retention time of 14.3 mL for ovalbumin (43 kDa), but consistent with that (13.2 mL) of BSA (67 kDa). The same results were obtained with the concentration of XPA as low as 0.03 mg/mL in the presence of 0.2 mg/mL of ribonuclease A (13.7 kDa) for the purpose of protein stabilization (data not shown). A linear regression of the data for the set of markers was then generated to calculate the molecular mass of XPA (Figure 3A). The nicely fitted standard line gave the XPA a molecular mass of 71 kDa that is well consistent with that of a XPA dimer. At least three independent experiments were performed for this determination. The data were very consistent as demonstrated in Figure 3 where the standard deviation error bars are too small to see as compared to the data symbols. The same experiments were also conducted on a Superdex-75 HR column, and the same results have been obtained, indicating the consistency of the determinations from different sizing columns. Since XPA protein contains seven cysteines, of which four are believed to form the zinc finger, we examined the XPA under limited denaturing conditions on a SDS−PAGE in the absence of reducing reagents to determine if any intermolecular disulfide bonds formed. The results indicated that there was no such kind of links involved (data not shown).

For comparison, we also investigated the gel filtration behavior of both the XPA and standard markers in the buffer containing 0.1% SDS on the same Superdex column (Figure 3B). Since the experiments were conducted under the denaturing conditions, proteins without disulfide bond cross-links should be in the form of monomer. As expected, analysis of the data indicated that the denatured XPA has an apparent molecular mass of 36.8 kDa (Figure 3B) that is consistent with the data from MS study (36.3 kDa). In contrast, the SDS−PAGE produced a molecular mass (43 kDa) significantly different from the 36.3 kDa value. This strongly supports the valid application of the gel filtration chromatography in this study.

PFO−PAGE Analysis. Recently, a new method called PFO−PAGE was developed to evaluate the oligomeric structure of proteins under native conditions (*12*). This method has been successfully used for both water-soluble and membrane proteins (*12*, *27*, *28*). Here, to verify the observation from the gel filtration chromatography, XPA protein together with the protein markers (catalase, BSA, and ovalbumin) was subjected to the PFO−PAGE analysis. As shown in Figure 4A, the band of XPA had a gel mobility shift corresponding to its dimeric form as compared to the markers. Also used as controls, the catalase (60 kDa per subunit) had a gel mobility shift corresponding to its native form of tetramer (232 kDa), while both BSA (66 kDa) and ovalbumin (43 kDa) were monomer as expected. In contrast, the XPA was clearly in its monomeric form when analyzed on SDS−PAGE (Figure 4B). The doublet of the XPA bands observed in the SDS−PAGE was generally reported before and was probably due to the intramolecular disulfide bonds formation during the electrophoresis (*15*).

Fluorescence Spectroscopy of XPA in PFO. The human XPA protein contains three fluorescent tryptophans located at 175, 194, and 235 residues, respectively, in the C-terminal half of the protein. Exposure of the internally buried tryptophans to the polar aqueous buffer on the protein surface usually results in a shift of the λ_{max} of fluorescence spectrum to the longer wavelength and a decrease in intensity. Therefore, changes in the environment of the tryptophans due to the protein structural alteration, may result in the characteristic changes of the fluorescence spectra of these fluorophores (*35*). The information of structural change may thus be obtained by determining the fluorescence properties of the protein under given experimental conditions. As shown in Figure 4C, the fluorescence spectra were measured for the XPA in the absence and the presence of 0.1 and 0.2% of PFO, as well as 6 M guanidine hydrochloride. The finding that the XPA in the absence and the presence of 0.1% PFO has a similar emission spectrum without wavelength shift implies that the protein has a similar structure under both conditions. In contrast, 0.2% PFO, which dissociates XPA into monomers as demonstrated by PFO−PAGE analysis (data not shown), produced a spectrum with a clear shift of the emission maximum to the longer wavelength (from 342 to 347 nm) and an apparent decrease in fluorescence intensity. The wavelength shift and the quenching indicated that some or all of the XPA tryptophans were in a more polar environment in the presence of 0.2% PFO, suggesting that an apparent conformational change of the protein may occur with more exposure of the tryptophan residues to the polar buffer. For comparison, the fluorescence of XPA in

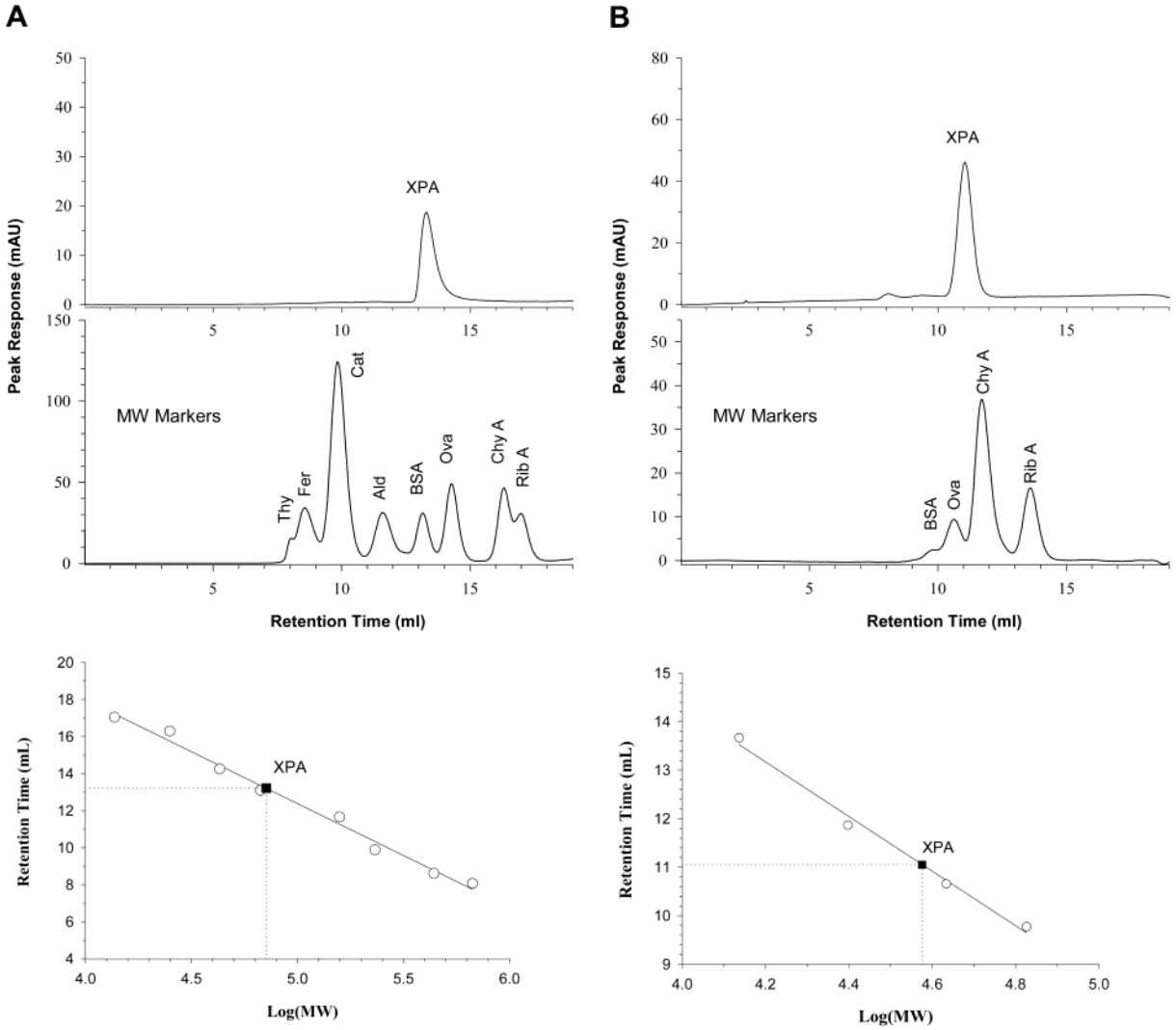

FIGURE 3: Gel filtration analysis of XPA. (A) XPA (200 μL, 0.3 mg/mL) and the molecular mass markers were gel-filtrated on a Superdex-200 HR column with the AKTApurifier (Amersham Pharmacia Biotech). The markers include Rib (ribonuclease A, 13.7), ChyA (chymotrysinogen A, 25), Ova (ovalbumin, 43), BSA (bovine albumin, 67), Ald (aldolase, 158), Cat (catalase, 232), Fer (ferritin, 440), and Thy (thyroglobulin, 669 kDa). The apparent molecular mass of XPA (71 kDa) was determined based on the relationship of the retention times of markers versus their molecular masses fitted with linear regression method. At least three independent experiments were performed and very consistent data were obtained, as the error bars representing the standard deviation plotted in the figure are too small to see in comparison to data symbols. (B) The similar experiments were performed under denaturing conditions in the presence of 0.1% SDS in both the running buffer and the sample. The molecular mass of denatured XPA (36.8 kDa) was determined based on the linear regression of the retention times of the four low molecular mass markers.

the presence of 6 M guanidine hydrochloride was also measured, in which the emission maximum shifted to a much longer wavelength of 355 nm (Figure 4C). Compared with this large shift for the denatured form of XPA, the shift from the XPA in the 0.2% PFO buffer suggests that the protein may still remain in a relatively folded structure. The red-shift of λ_{max} for the XPA in the 0.2% PFO may be due to the loss of the quaternary structure of the protein (dimer) with some of the tryptophans located in the dimerization interface. This is consistent with the conclusion that XPA exists as a dimer. The shift from 347 to 355 in the presence of guanidine chloride is likely the result of destruction of secondary and tertiary structures of the protein.

Analysis of XPA-XPA Binding. In this protein−protein binding assay, two different recombinant human XPA proteins were overproduced with the pTYB−XPA and the recombinant baculovirus pBac-XPA in *E. coli* and insect cells, respectively. The XPA produced from pTYB−XPA (Eco−XPA) has an original molecular mass of 32 kDa. In contrast, the XPA from pBac−XPA (Bac−XPA) has a molecular mass of 36 kDa due to an N-terminal tag. In addition, the pTYB−XPA originally generates a chitin binding domain (CBD)-fused XPA protein, which binds tightly to the chitin-beads column. Subsequent incubation with high concentration of DTT (30 mM) after thorough wash of the column triggers the cleavage of the XPA protein (32 kDa) from the CBD. Since these XPA proteins of different sizes are well separated on SDS−PAGE (lanes 1 and 2, Figure 5), the potential binding between these two proteins can be examined. Specifically, before binding to the chitin beads on the column, the supernatant of the pTYB−XPA overexpressed *E. coli* cells was incubated with the purified XPA from pBac-XPA infected insect cells to allow the two types of XPA proteins to exchange with one another (see Experimental Procedures). As a control, the purified Bac-XPA was also mixed with the supernatant of

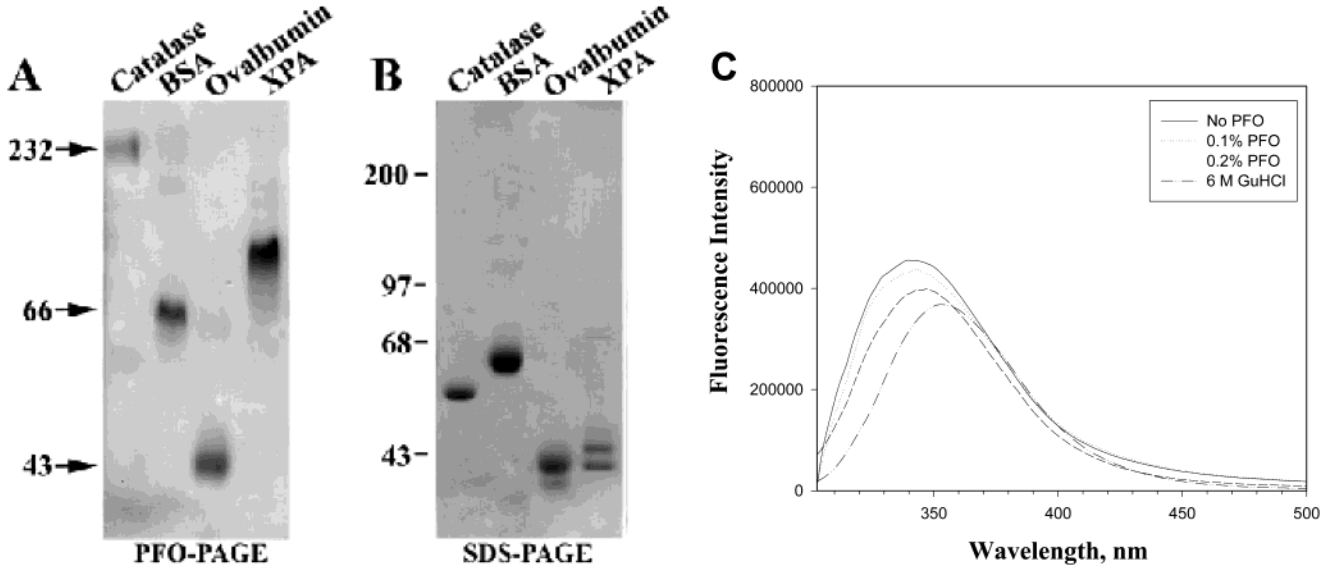

FIGURE 4: PFO−PAGE Analysis of XPA. (A) Two micrograms each of catalase (tetramer, 232 kDa), BSA (66 kDa), and ovalbumin (43 kDa), and purified XPA were solubilized in PFO and separated on a 7.5% native PFO−PAGE at 4 °C. The XPA migrated with a shift corresponding to the molecular mass of homodimer. (B) The same proteins were solubilized in SDS and separated on a regular 7.5% SDS−PAGE. The XPA migrated with a size of monomer. (C) The fluorescence spectra of XPA in the absence and presence of PFO were recorded with the excitation at 295 nm. The XPA was in the buffer of 25 mM Tris, 192 mM glycine at pH 8.5, with different concentrations of NaPFO and 6 M guanidine hydrochloride.

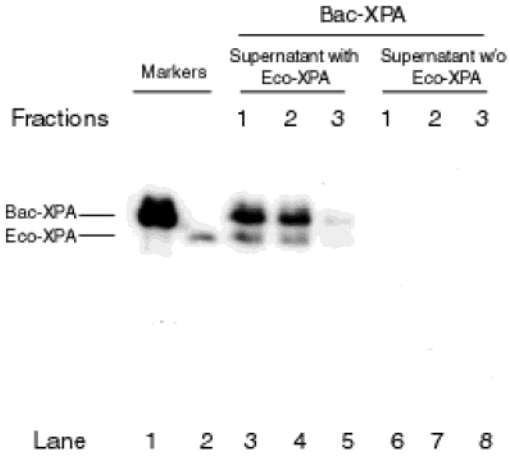

FIGURE 5: Binding of pTYB−XPA produced human XPA with the human XPA generated from pBac-XPA analyzed by Western blotting. Lanes 3−5, fractions eluted from the chitin column loaded with the preincubated mixture of the *E. coli* pLysS cell supernatant overexpressing the pTYB−XPA and the purified pBac-XPA generated XPA (Bac-XPA). Lanes 6−8, fractions eluted from the chitin column loaded with the preincubated mixture of the *E. coli* pLysS cell supernatant without pTYB−XPA and the pBac-XPA generated XPA (Bac-XPA). The pTYB−XPA produced XPA from *E. coli* cells (Eco-XPA) has a molecular mass of 32 kDa (lane 2) and the Bac-XPA is a protein of 36 kDa. A monoclonal antibody against XPA was used for the probing.

E. coli cells without pTYB−XPA following the same procedures. After the binding and extensive washing, only CBD-Eco-XPA and its associated proteins are expected to remain bound to the chitin column. As shown in Figure 5, in comparison with the control (lanes 6−8), bands corresponding to the Bac−XPA protein were identified in the Western blotting analysis of the eluted fractions after the DTT cleavage of the proteins from the column (lanes 3−5). The results strongly suggest that the Bac−XPA forms a complex with the Eco−XPA, and therefore the dimerization of XPA most likely occurred.

Interaction of XPA with RPA. In human NER, XPA interacts with RPA to form a complex that functionally recognizes damaged DNA. Therefore, it is of great interest to examine the stoichiometry of the XPA−RPA protein complex. As shown in Figure 6, the RPA protein (0.61 μM) was titrated with varying concentrations of XPA and analyzed by the gel filtration chromatography on the Superdex-200 HR column. In Figure 6, the XPA and RPA proteins were essentially well-separated from each other through the column, though some extent of overlapping did occur. For comparison, the similar experiments were also carried out for the XPA at the same concentrations in the absence of RPA, which generated a linear relationship of the absorption (280 nm) versus the concentrations. The data in Figure 6 showed that in the absence of XPA, the RPA is featured by a dominant peak with a retention time of 11.6 mL, corresponding to the association of p70, p32, and p14 subunits of RPA. Two minor peaks were also observed, one at 12.5 mL and the other at 14.1 mL. Those are due to the partial degradation of RPA, and the complex formation between the p32 and p14 subunits, respectively (*16*, *17*), as supported by a SDS−PAGE analysis of the fractions (data not shown). Addition of enough amount of XPA to the RPA produced a separate new absorption maximum at 13.1 mL (Figure 6A), which was contributed by the unbound XPA as confirmed by SDS−PAGE (data not shown). However, at the concentrations of XPA lower than 1.22 μM (XPA/RPA = 2), little or no free XPA was observed at 13.1 mL, indicating that the XPA molecules were bound to RPA. As shown in Figure 6, even at 1.22 μM, only very small absorption intensity for free XPA was detected over the background, as compared to the intensity for the XPA at the same concentration in the absence of RPA (right panel of Figure 6A). Therefore, the increasing absorption peak of the free XPA served as the signal to be monitored during the titration. The intensity corresponding to the unbound XPA was calculated based on the integrated area under each of the titration-generated

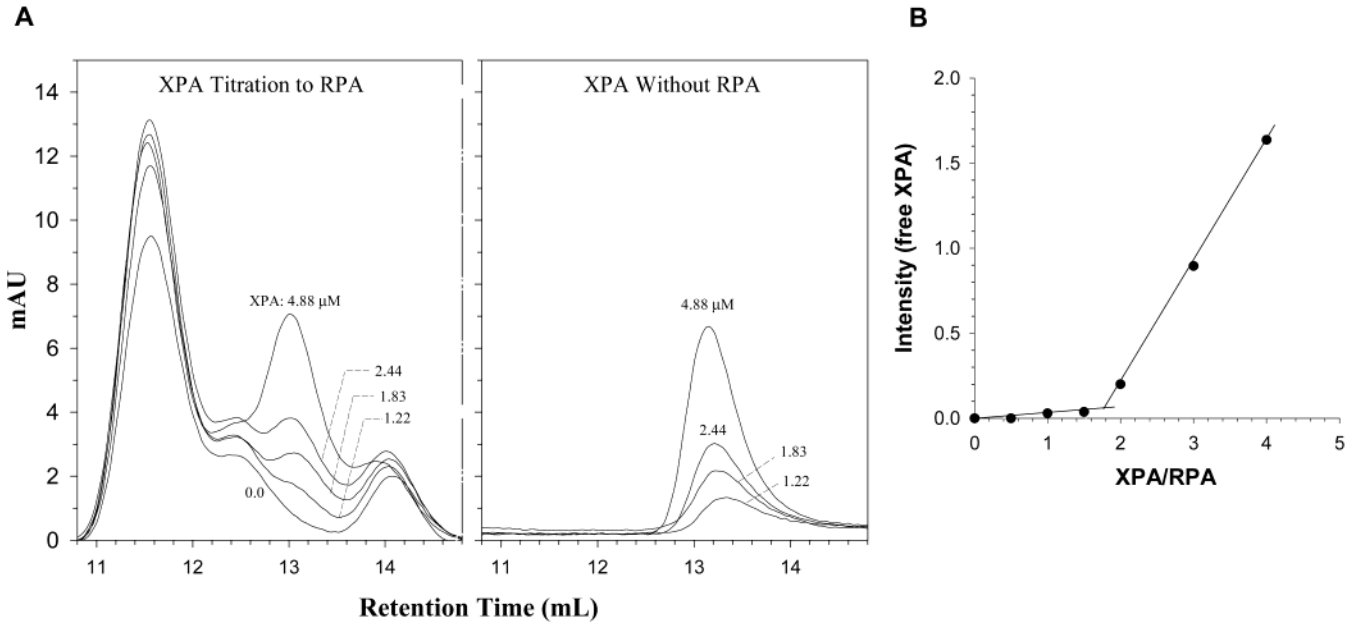

FIGURE 6: Interaction of XPA with RPA. (A) RPA (0.61 μM) incubated with different concentrations of XPA at room temperature for 15 min was analyzed on a Superdex-200 HR column with the AKTApurifier system (Amersham Pharmacia Biotech). In comparison, the gel filtration of the XPA with the same concentrations in the absence of RPA was also performed. The curve with the zero concentration of XPA represents the gel filtration for RPA. The peaks with the indication of XPA concentration represent the free or unbound XPA. (B) The binding isotherm was generated by plotting the intensity of free-XPA absorption (280 nm) as a function of the total molar ratio of XPA/RPA. The ratio at the crossing point of the two best-fitted lines of the binding isotherms gave the stoichiometry of the binding, suggesting that each RPA binds to two XPA molecules.

peaks over the background, and then plotted as a function of the total molar ratio of XPA/RPA (Figure 6B). Since the concentration of RPA (0.61 μM) was much higher than the dissociate constant (~19 nM) for XPA binding to RPA (*26*), the stoichiometry of this binding was estimated from the value of XPA/RPA at the crossing point of the two best-fitted lines of the binding isotherms. The value was about 1.8, suggesting that the interaction of XPA with RPA resulted in the formation of the XPA_2−RPA protein complex. In addition, the experimental binding isotherms were nicely fitted with a nonlinear least-squares method using the 2:1 binding model (*39*) (data not shown).

It should be mentioned that, in Figure 6A, the RPA peak did not shift to the left upon the addition of XPA. This is probably because that the RPA may contain a large hollow structure which is able to accommodate the major part of the XPA molecule. RPA is a protein of three subunits, p70, p32, and p14, which most likely form a nonglobular protein. This is consistent with the retention time of RPA from the gel filtration experiment, which corresponds to a molecular mass of ~170 kDa, a value much higher than the actual molecular mass of 116 kDa for RPA. This subject is currently under investigation.

DISCUSSION

The importance of XPA in human cells is illustrated by its indispensable roles in NER including both GGR and TCR. It has been generally accepted that XPA is a DNA damage recognition protein directly involved in the early steps and probably also the late steps of NER. These functions of XPA are delivered by its interactions with other NER proteins and with the damaged DNA. Understanding of these interactions depends on the availability of the basic information on the molecular composition of XPA, which decisively affects the interactions. Instead, XPA has been widely assumed to be a monomer acting in the mechanism of NER. In the present study, data obtained using three independent approaches suggested that the functional form of XPA is a homodimer.

The use of gel filtration chromatography for determination of protein molecular mass is well documented. Although the retention time of gel filtration directly corresponds to the size of the protein and thus the shape of the protein may affect the relationship between the retention time and molecular mass, the effect is limited in most cases of proteins. Upon the gel filtration determination, the result was then confirmed by the native PFO−PAGE assay and fluorescence spectroscopic analysis. Our results are also consistent with a previous observation of *Xenopus* XPA oligomerization in a glutaraldehyde cross-linking experiment (*15*). In human NER, XPA works together with RPA, a complex of three subunits, to recognize the damaged DNA (*8*). The knowledge of the functional form of XPA in the complex with RPA could be important for understanding the structure−function aspects of the complex. The data from our titration analysis indicated that the dimer rather than the monomer of XPA forms complex with RPA, which in another way verified the dimerization of XPA. Interestingly, by examining the recent data presented by Missura et al. in their inhibition study of DNA unwinding (*8*), it also appears that XPA may have a binding ratio to RPA about two, although the authors did not mention this possibility in their report.

In nucleotide excision repair, other known initial DNA damage recognition proteins such as $UvrA_2$ in *E. coli*, XPC−HR23B, and RPA, are either homodimer, heterodimers, or heterotrimers. The oligomerization of these proteins may provide the necessary structures for protein binding to DNA, or recognizing DNA structural alterations and lesions. In the *E. coli* NER system, each UvrA molecule has two zinc

fingers and is primarily involved in the first step of damage recognition for detecting the DNA conformational changes from Watson−Crick structure induced by DNA lesions (*32*, *33*). Interestingly, XPA was also recently identified as the damage recognition protein specifically sensing the DNA bending and unwinding (*8*). It is, therefore, not surprising that XPA is also a dimer if at least two zinc fingers are required for probing such DNA structural alterations.

One of the direct effects of the XPA dimerization on our understanding of the mechanism of human NER is regarding to the XPA binding to the damaged DNA in the damage recognition process. Our results suggest that the dimerization needs to be considered in the evaluation of the binding constants. Correct determination of these biochemical properties is critical for defining the activities of the XPA in NER and may also be helpful in addressing the contradictory results in the mechanistic actions of XPA and XPC in NER (*18*). Previously, the binding affinity of XPA for DNA damage has been widely measured and used as a strong evidence for the role of XPA in damaged or damage-induced DNA abnormal structure recognition (*9*, *10*, *19*, *20*). In addition, the knowledge of XPA dimerization may also help us understand the molecular structures of the XPA−DNA interactions. Although the NMR studies of DNA binding domain of XPA have shown that XPA contains an accommodative domain structure for docking double-stranded DNA (*21*, *22*), a full structural understanding of the interaction of XPA with DNA may need to include the XPA dimerization. And this may be also true when the interactions of XPA with other NER proteins are concerned, such as its interactions with RPA, XPF-ERCC1, and TFIIH (*23*−*31*).

ACKNOWLEDGMENT

We thank Drs. Istvan Boldogh and Bo Xu (University of Texas Medical Branch) for their helps in obtaining XPA protein and in the initial setup of the gel filtration experiments, respectively. We are grateful to Dr. Ashis Basu (University of Connecticut) for graciously providing the AAF-adducted DNA 11mer. We acknowledge Dr. T. Haag and Z. Wu (University of Texas Medical Branch) for their help in obtaining mass spectroscopy. We thank Jack Ma for his help in obtaining fluorescence spectroscopy data. We acknowledge National Cell Culture Center for providing service on baculovirus propagation and infected cell production.

REFERENCES

1. Sancar A. (1996) *Annu. Rev. Biochem. 65*, 43−81.
2. Wood, R. D. (1996) *Annu. Rev. Biochem. 65*, 135−167.
3. Hanawalt, P. C. (1994) *Science 266*, 1957−1958.
4. de Laat, W. L., Jaspers, N. G., and Hoeijmakers, J. H. (1999) *Genes Dev. 13*, 768−785.
5. Li, L., Elledge, S. J. Peterson, C. A., Bales, E. S., and Legerski, R. J. (1994) *Proc. Natl. Acad. Sci. U.S.A. 91*, 5012−5016.
6. Park, C. H., and Sancar, A. (1994) *Proc. Natl. Acad. Sci. U.S.A. 91*, 5017−5021.
7. Nocentini, S., Coin, F., Saijo, M., Tanaka, K., and Egly, J.-M. (1997) *J. Biol. Chem. 272*, 22991−22994.
8. Missura, M., Buterin, T., Hindges, R., Hubscher, U., Kasparkova, J., Brabec, V., and Naegeli, H. (2001) *EMBO J. 20*, 3554−3564.
9. Burns, J. L., Guzder, S. N., Sung, P., Prakash, S., and Prakash, L. (1996) *J. Biol. Chem. 271*, 11607−11610.
10. Wakasugi, M., and Sancar, A. (1999) *J. Biol Chem. 274*, 18759−18768.
11. Sugasawa, K., Ng, J. M. Y., Masutani, C., Iwai, S., van der Spek, P. J., Eker, A. P. M., Hanaoka, F., Bootsma, D., and Hoeijmakers, J. H. J. (1998) *Mol. Cell. 2*, 223−232.
12. Ramjeesingh, M., Huan, L.-J., Garami, E., and Bear, C. E. (1999) *Biochm. J. 342*, 119−123.
13. Ariza, R. R., Keyse, S. M., Moggs, J. G., and Wood, R. D. (1996) *Nucleic Acids Res. 24*, 433−440.
14. Hermanson, I. L., and Turchi, J. J. (2000) *Protein Expression Purif. 19*, 1−11.
15. Iakoucheva, L. M., Kimzey, A. L., Masselon, C. D., Smith, R. D., Dunker, A. K., and Ackerma, E. J. (2001) *Protein Sci. 10*, 1353−1362.
16. Wold M. S., and Kelly, T. (1988) *Proc. Natl. Acad. Sci. U.S.A. 85*, 2523−2527.
17. Henricksen, L. A., Umbricht, C. B., and Wold, M. S. (1994) *J. Biol Chem. 269*, 11121−11132.
18. Wood, R. D. (1999) *Biochimie 81*, 39−44.
19. Jones, C. J., and Wood, R. D. (1993) *Biochemistry 32*, 12096−12104.
20. Asahina, H., Kuraoka, E., Shirakawa, M., Morita, E. H., Miura, N., Miyamoto, I., Ohtsuka, E., Okada, Y., and Tanaka, K. (1994) *Mutat. Res. 315*, 229−237.
21. Ikegami, T., Kuraoka, I., Saijo, M., Kodo, N., Kyogoku, Y., Morikawa, K., Tanaka, K., Shirakawa, M. (1998) *Nat. Struct. Biol. 5*, 701−706.
22. Buchko, G. W., Daughdrill, G. W., de Lorimier, R., Rao, B. K., Isern N. G., Lingbeck, J. M., Taylor, J. S., Wold, M. S., Gochin, M., Spicer, L. D., Lowry, D. F., Kennedy, M. A. (1999) *Biochemistry 38*, 15116−15128.
23. He, Z., Henricksen, L. A., and Wold M. S. (1995) *Nature 374*, 566−569.
24. Li, L., Lu, X., Peterson, C. A., and Legerski, R. J. (1995) *Mol. Cell. Biol. 15*, 5396−5402.
25. Park, C.-H., Mu, D., Reardon, J. T., and Sancar, A. (1995) *J. Biol. Chem. 270*, 4896−4902.
26. Saijo, M., Kuraoka, I., Masutani, C., Hanaoka, F., and Tanaka, K. (1996) *Nucleic Acids Res. 24*, 4719−4724.
27. Kedei, N., Szabo, T., Lile, J. D., Treanor, J. J., Olah, Z., Iadarola, M. J., and Blumberg, P. M. (2001) *J. Biol. Chem. 276*, 28613−28619.
28. Ramjeesingh, M., Li, C., Huan, L. J., Garami, E., Wang, Y., and Bear, C. E. (2000) *Biochemistry 39*, 13838−13847.
29. Li, L., Peterson, C. A., Lu, X., and Legerski, R. J. (1995) *Mol. Cell. Biol. 15*, 1993−1998.
30. Nagai, A., Saijo, M., Kuraoka, I., Matsuda, T., Kodo, N., Nakatsu, Y., Mimaki, T., Mino, M., Biggerstaff, M., Wood, R. D., Sijbers, A., Hoeijmakers, J. H. J., and Tanaka, K. (1995) *Biochem. Biophys. Res. Commun. 211*, 960−966.
31. Morikawa, K., and Shirakawa, M. (2000) *Mutat. Res. 460*, 257−275.
32. Zou, Y., and Van Houten, B. (1999) *EMBO J. 18*, 4889−4901.
33. Zou, Y., Luo, C., and Geacintov, N. (2001) *Biochemistry 40*, 2923−2931.
34. Luo, C., and Krishnasamy, R., Basu, A. K., and Zou, Y. (2000) *Nucleic Acids Res. 28*, 3719−3724.
35. Lakowicz, J. R. (1999) *Principle of Fluorescence Spectroscopy*, Kluwer Academic/Plenum Press, New York.
36. Volker, M., Mone, M. J., Karmakar, P., van Hoffen, A., Schul, W., Vermeulen, W., Hoeijmakers, J. H. J., van Driel, R., van Zeeland, A. A., and Mullenders, L. H. F. (2001) *Mol. Cell 8*, 213−224.
37. Zou, Y., Crowley, D. J., and Van Houten, B. (1998) *J. Biol. Chem. 273*, 12887−12892.
38. Patrick S. M., and Turchi, J. J. (1999) *J. Biol. Chem. 274*, 14972−14978.
39. Zou, Y., Bassett, H., Walker, R., Bishop, A., Amin, S., Geacintov, N. E., and Van Houten, B. (1998) *J. Mol. Biol. 281*, 107−119.

BI026064Z